

1 **The clinical utility of two high-throughput 16S rRNA gene sequencing**
2 **workflows for taxonomic assignment of unidentifiable bacterial pathogens in**
3 **MALDI-TOF MS**

4 Hiu-Yin LAO^a, Timothy Ting-Leung NG^a, Ryan Yik-Lam WONG^b, Celia Sze-Ting
5 WONG^b, Chloe Toi-Mei CHAN^a, Denise Sze-Hang WONG^a, Lam-Kwong LEE^a
6 Stephanie Hoi-Ching JIM^a, Jake Siu-Lun LEUNG^a, Hazel Wing-Hei LO^a, Ivan Tak-Fai
7 WONG^a, Miranda Chong-Yee YAU^b, Jimmy Yiu-Wing LAM^b, Alan Ka-Lun WU^b,
8 Gilman Kit-Hang SIU^{a#}

9

10 ^a *Department of Health Technology and Informatics, The Hong Kong Polytechnic University,*
11 *Hong Kong Special Administrative Region, China*

12 ^b *Department of Clinical Pathology, Pamela Youde Nethersole Eastern Hospital, Hong Kong*
13 *Special Administrative Region, China*

14

15 # Correspondence author: Dr. Gilman KH SIU, Department of Health Technology and
16 Informatics, Hong Kong Polytechnic University, Hong Kong (gilman.siu@polyu.edu.hk)

17

18

19 **ABSTRACT**

20 Bacterial pathogens that cannot be identified using matrix-assisted laser desorption/ionization
21 time-of-flight mass spectrometry (MALDI-TOF MS) are occasionally encountered in clinical
22 laboratories. The *16S rRNA* gene is often used for sequence-based analysis to identify these
23 bacterial species. Nevertheless, traditional Sanger sequencing is laborious, time-consuming and
24 low-throughput. Here, we compared two commercially available *16S rRNA* gene sequencing
25 tests, which are based on Illumina and Nanopore sequencing technologies, respectively, in their
26 ability to identify the species of 172 clinical isolates that failed to be identified by MALDI-TOF
27 MS. Sequencing data were analyzed by respective built-in analysis programs (MiSeq Reporter
28 Software and Epi2me) and BLAST+ (v2.11.0). Their agreement with Sanger sequencing on
29 species-level identification was determined. Discrepancies were resolved by whole-genome
30 sequencing. The diagnostic accuracy of each workflow was determined using the composite
31 sequencing result as the reference standard. Despite the high base-calling accuracy of Illumina
32 sequencing, we demonstrated that the Nanopore workflow had a comparatively higher taxonomic
33 resolution at the species level. Using built-in analysis algorithms, the concordance of Sanger 16S
34 with the Illumina and Nanopore workflows was 33.14% and 87.79%, respectively. The
35 agreement was 65.70% and 83.14%, respectively, when BLAST+ was used for analysis.
36 Compared with the reference standard, the diagnostic accuracy of optimized Nanopore 16S was
37 96.36%, which was identical to Sanger 16S and was better than Illumina 16S (71.52%). The
38 turnaround time of the Illumina workflow and the Nanopore workflow was 78h and 8.25h,
39 respectively. The per-sample cost of the Illumina and Nanopore workflows was US\$28.5 and
40 US\$17.7, respectively.

41

42

43 **INTROUDUCTION**

44 Traditionally, clinical microbiology laboratories have relied on phenotypic methods to identify
45 bacterial pathogens. However, conventional biochemical tests are labor-intensive and time-
46 consuming, and the results can be ambiguous when two species share similar biochemical
47 profiles (1, 2). Nowadays, matrix-assisted laser desorption/ionization time-of-flight mass
48 spectrometry (MALDI-TOF MS) is widely used for bacterial identification in clinical
49 laboratories (3). MALDI-TOF MS allows rapid identification of microorganisms by comparing
50 the mass spectrum of a sample with the reference spectra in the database (4). Although MALDI-
51 TOF MS is a rapid, simple and high-throughput technology for bacterial identification, some
52 species cannot be well differentiated due to high similarity in the mass spectra of closely related
53 species or lack of reference spectra (5).

54 A study from Lau *et al.* reported that MALDI-TOF MS failed to determine the species of over
55 70% of phenotypically “difficult-to-identify” bacteria in clinical laboratories(6). In general,
56 anaerobes, particularly *Actinomyces* spp., *Peptostreptococcus* spp., *Prevotella* spp. and
57 *Fusobacterium* spp. (7-9), have a higher failure rate compared with aerobes in bacterial
58 identification using MALDI-TOF MS (7, 10). Additionally, some Gram-positive aerobes, such
59 as *Nocardia* spp. and *Streptomyces* spp., are poorly identified by MALDI-TOF MS (7, 11).
60 Regarding Gram-negative aerobes, studies show that MALDI-TOF MS cannot effectively
61 identify *Acinetobacter* spp., *Chryseobacterium* spp. and *Moraxella* spp. at the species level (11,
62 12). In such cases, *16S* sequencing of cultured isolates is commonly used for species-level
63 identification.

64 Sanger sequencing offers a high base-calling accuracy, but it is laborious and time-consuming
65 with limited throughput (13). High-throughput sequencing (HTS) technologies have been
66 proposed as alternatives to generate *16S* sequences for rapid identification of bacteria that are of
67 clinical interest. Next-generation sequencing (NGS), such as can be achieved using Illumina
68 platforms, can generate vast quantities of accurate sequencing reads. However, the read length is
69 limited and insufficient to cover the entire *16S* rRNA gene. According to the official workflow
70 for *16S* rRNA sequencing developed by Illumina Ltd., bacteria are identified based on variable
71 regions (V3 and V4) of *16S*. Nevertheless, these regions are not equally discriminative between
72 and across different species, genera and families (14).

73 The MinION device by Oxford Nanopore Technologies (ONT) enables generation of reads
74 exceeding 30 kb. The official *16S* rRNA sequencing assay allows the entire *16S* rRNA gene to
75 be sequenced with real-time data analysis. Recent studies have demonstrated its potential for
76 rapid bacterial identification; however, the high read-error rate (8%–15%) of this platform might
77 hinder the accuracy of species-level identification for diagnostic purposes (15).

78 Considering the respective limitations of Illumina and Nanopore technologies, a comprehensive
79 investigation of the clinical utility of these *16S* rRNA sequencing approaches for bacterial
80 identification is required. This study aimed to evaluate the performance of two commercial HTS
81 workflows for *16S* rRNA sequencing, namely the 16S Metagenomic Sequencing Library
82 Preparation workflow (Nextera XT Index kit v2) from Illumina and the 16S Barcoding Kit 1-24
83 (SQK-16S024) from ONT, coupled with the respective built-in analysis programs and in-house
84 BLAST+ (v2.11.0) analysis. These workflows were used to identify bacterial isolates that could
85 not be differentiated by MALDI-TOF MS. In light of the complexities of evaluating diagnostic
86 accuracy in the absence of a perfect gold standard, we considered a composite *16S* rRNA

87 sequencing result inferred by Sanger and the two HTS platforms as a reference standard. In case
88 of disagreement in taxa inferred by the three sequencing platforms, whole-genome sequencing
89 (WGS) was conducted to confirm the bacterial identities. In addition, the cost and time-to-result
90 of the sequencing workflows were also compared.

91

92 MATERIALS AND METHODS

93 **Sample collection and preparation**

94 A total of 172 clinical isolates from 117 species were collected from the clinical microbiology
95 laboratory of Pamela Youde Nethersole Eastern Hospital. Clinical isolates were included if they
96 failed to be classified at the species level (score < 2.00) by the IVD MALDI Biotyper (Bruker
97 Daltonics, Bremen, Germany). Failure to identify bacterial species occurred due to (i) lack of a
98 reference spectrum in the database (81 samples); (ii) inclusion of certain species in the
99 “dangerous database,” named Security Library 1.0, rather than the regular database (two
100 samples); or (iii) poor-quality samples (89 samples) (Table S1). The IVD MALDI Biotyper used
101 in this study was microflex[®] (Bruker Daltonics), and the database version was BD-6763.

102 Total nucleic acid was extracted from clinical isolates using the AMPLICOR[®] Respiratory
103 Specimen Preparation Kit (Roche, Basel, Switzerland) and purified with 1.8X AMPure XP beads
104 (Beckman Coulter, California, USA). Purified DNA was diluted to targeted concentrations in
105 subsequent sequencing workflows. The required DNA input for the Illumina and Nanopore
106 workflows was 12.5 ng and 10 ng, respectively.

107

108 **Sanger *16S* rRNA sequencing (Sanger *16S*)**

109 The full-length *16S* rRNA gene was amplified using primers for 16s_008F (5'-
110 AGAGTTTGATCMTGGC-3') and 16s_1507R (5'-TACCTTGTTACGACTT-3') (16). The
111 reaction mixture was prepared by mixing 36.7 µl of nuclease-free water, 5 µl of 10× polymerase
112 chain reaction (PCR) buffer, 1 µl of 10-mM deoxynucleoside triphosphate mix (NEB, Ipswich,
113 Massachusetts, USA), 1 µl of each 25-µM primer, 0.3 µl of HotStarTaq Plus DNA Polymerase
114 (Qiagen, Hilden, Germany) and 5 µl of DNA template. The PCR conditions were 96°C for 8
115 min, 37 cycles at 94°C for 1 min, 37°C for 2 min and 72°C for 2 min 30 s, followed by 72°C for
116 10 min, and a hold step at 4°C. PCR products were purified using ExoSAP-IT reagent (Thermo
117 Fisher Scientific, Waltham, MA, USA) and then passed to the subsequent cycle sequencing using
118 eight sequencing primers (17-19) (Table S2). The reaction mixture consisted of 13 µl of
119 nuclease-free water, 1 µl of BigDye[®] Terminator v3.1 Ready Reaction Mix (Thermo Fisher
120 Scientific), 3.5 µl of 5× sequencing buffer, 1 µl of 3.2-µM primer and 1.5 µl of purified PCR
121 product. The PCR conditions were 96°C for 1 min, 25 cycles at 96°C for 10 sec, 37°C for 30 sec
122 and 60°C for 4 min, followed by a hold step at 4°C. The sequencing products were purified using
123 75% isopropanol and resuspended in 12 µl of Hi-Di[™] Formamide (Thermo Fisher Scientific).
124 After loading on the Applied Biosystems[®] 3130 Genetic Analyzer (Thermo Fisher Scientific),
125 the resulting raw trace files were analyzed using the Staden Package (v2.0.0b11). The consensus
126 sequence of each sample was classified by submitting a Basic Local Alignment Search Tool
127 (BLAST) query against the *16S* ribosomal RNA sequence database.

128

129 **Illumina sequencing (NGS *16S*)**

130 **Library preparation.** Libraries were constructed according to the 16S Metagenomic Sequencing
131 Library Preparation workflow from Illumina. Briefly, the *16S* V3 and V4 regions of samples

132 were amplified in the first stage of PCR using the primers suggested in the workflow, which
133 were 16S Amplicon PCR Forward Primer (5'-
134 TCGTCGGCAGCGTCAGATGTGTATAAGAGACAGCCTACGGGNGGCWGCAG-3') and
135 16S Amplicon PCR Reverse Primer (5'-
136 GTCTCGTGGGCTCGGAGATGTGTATAAGAGACAGGACTACHVGGGTATCTAATCC-
137 3'). The underlined bases in the primer sequences are the overhang adapter sequences for
138 attachment of the indexed adapters in the second stage of PCR. The size of the amplicon was
139 approximately 460 bp. After a post-PCR clean-up, a unique indexed sequencing adapter was
140 added to each sample using the Nextera XT Index kit v2 (Illumina, San Diego, California, USA).
141 Then, a second post-PCR clean-up was performed, followed by a qualification check of the
142 purified libraries.

143 ***Quantification and sequencing.*** The size of each library was measured using the 2100
144 Bioanalyzer system (Agilent, Santa Clara, CA, USA) and the High Sensitivity DNA kit
145 (Agilent). The quantity of the libraries was measured by real-time PCR using the LightCycler®
146 480 Instrument II (Roche) and QIAseq™ Library Quant Assay Kit (Qiagen). Then, the libraries
147 were diluted to 4 nM and pooled into one tube. After denaturation with 0.2-N NaOH, the pooled
148 library was diluted to 9 pM and spiked with 15% of 9-pM PhiX prepared from PhiX Control Kit
149 v3 (Illumina). The pooled library was then loaded on the MiSeq sequencer (Illumina) for
150 sequencing using MiSeq Reagent Kits v3 (Illumina). The sequencing time was 56 h.

151 ***On-instrument data analysis.*** Sequencing data were analyzed using MiSeq Reporter software
152 (v2.6.2.3) (MSR) in the MiSeq system. After selecting the metagenomics workflow, sequencing
153 reads were mapped against reference sequences in the Greengenes database (v13.5, May 2013)

154 (<http://greengenes.lbl.gov/>) for classification. The classification of reads at seven taxonomic
155 levels from kingdom to species was analyzed in this workflow.

156 **Data analysis using NGS_BLAST+**. The paired-end reads of each sample were merged using
157 the “make.contigs” command in Mothur (v1.44.3) (20). The reads were filtered using the
158 “screen.seqs” command. Sequences smaller than 400 bp, larger than 500 bp, or with any
159 ambiguous bases were removed. The resulting fasta files were analyzed by BLAST+ (v2.11.0)
160 using an in-house Python script
161 (https://github.com/siupenyau/Pocket_16S/tree/7d3fa9d73a6a35afb47e40e7850cef72b4b91a22).

162 In brief, the reads were aligned to the reference sequences in the *16S* ribosomal RNA database
163 (<https://ftp.ncbi.nlm.nih.gov/blast/db/>) downloaded from the National Center for Biotechnology
164 Information (NCBI). The percentage identity and percentage query coverage were set at 90%.

165

166 **Nanopore sequencing (Nanopore *16S*)**

167 **Library preparation and sequencing.** Library preparation was performed using the 16S
168 Barcoding Kit 1-24 (SQK-16S024) from ONT according to the manufacturer’s protocol.
169 Libraries were quantified using the Qubit 2.0 Fluorometer (Thermo Fisher Scientific) with the
170 Qubit™ 1X dsDNA HS Assay Kit (Thermo Fisher Scientific). Then, 24 barcoded libraries were
171 pooled into one tube in equal concentrations. After ligation with the rapid adapter, sequencing
172 was performed using the flow cell FLO-MIN106 R9.4.1 with the MinION sequencer on the
173 MinKNOW platform for approximately 4 h.

174 **On-instrument real-time data analysis.** During sequencing, the passed fastq files, which had a
175 quality score of >7, were uploaded on the cloud-based data analysis platform Epi2me for

176 analysis. Sequencing reads were aligned to reference sequences in the NCBI 16S bacterial
177 database using the FASTQ 16S workflow (v2020.04.06). Regarding the workflow parameters,
178 the minimum QSCORE was set at 7, while the minimum percentage coverage and minimum
179 percentage identity were set at 90%.

180 **Data analysis using NanoBLAST+.** In addition to Epi2me, sequencing data were analyzed using
181 BLAST+ (v2.11.0), similar to the analysis of NGS data. As each sample generated multiple fastq
182 files in a sequencing run, the fastq files of each sample were first merged into a single fastq file
183 and then converted to a fasta file before being aligned to reference sequences in the database.

184 **Data analysis using NanoCLUST.** Samples with disagreement between EPI2ME and
185 NanoBLAST+ were further analyzed using another pipeline, NanoCLUST
186 (<https://github.com/genomicsITER/NanoCLUST>) (21). Unlike Epi2me and NanoBLAST+,
187 NanoCLUST does not classify individual reads in a sample. Instead, NanoCLUST forms clusters
188 of similar reads and classifies the consensus sequence of each cluster.

189 **Whole genome sequencing (WGS)**

190 Samples with complete discordant taxa, as inferred by Sanger 16S, NGS 16S and Nanopore 16S
191 tests, were subjected to WGS to confirm the definite identities using the ONT platform. Library
192 preparation was performed using the transpose-based rapid barcoding kit (SQK-RBK110.96)
193 according to the manufacturer's protocol. After pooling and adapter ligation, the library was
194 loaded on the flow cell FLO-MIN106 R9.4.1 and sequenced using the GridION device for 48 h
195 in high-accuracy base calling mode. The passed fastq files were uploaded to Epi2me and
196 analyzed using the WIMP workflow (v2021.03.05).

197 **De novo assembly for WGS datasets**

198 Sequencing reads of each sample were assembled using Shasta (v0.7.0)
199 (<https://github.com/chanzuckerberg/shasta>). Sequencing reads were re-aligned to the assembled
200 consensus sequences using minimap2 (v2.17-r941) and samtools (v1.10). Consensus sequences
201 were first polished using MarginPolish (v1.3.dev-5492204) ([https://github.com/UCSC-nanopore-](https://github.com/UCSC-nanopore-cgl/MarginPolish)
202 [cgl/MarginPolish](https://github.com/UCSC-nanopore-cgl/MarginPolish)) and then further polished using homopolish (v0.2.1)
203 (<https://github.com/ythuang0522/homopolish>) (22). To avoid bioinformatic bias in de novo
204 assembly, each sample was also subjected to a second analysis pipeline. In brief, the sequencing
205 reads were assembled using miniasm (v0.3-r179)
206 (<https://github.com/lh3/miniasm/releases/tag/v0.3>). All-vs-all read self-mapping was performed
207 using minimap2. Raw consensus sequences were then generated using miniasm. After re-
208 alignment of the raw reads to consensus sequences using minimap2, the consensus sequences
209 were polished twice using racon (v1.4.3) (<https://github.com/isovic/racon>).

210 The longest polished consensus sequences of each sample were classified using BLAST+
211 (v2.11.0) with the Prokaryotic RefSeq Genomes database downloaded from the NCBI. The top
212 classified species with both query coverage and percentage identity were reported. The average
213 nucleotide identity (ANI) between the query and best-matched reference genomes was calculated
214 using an ANI calculator (<https://www.ezbiocloud.net/tools/ani>) (23). ANI >94% indicated that
215 the samples belong to the same species as the best-matched genomes.

216 **Data and statistical analysis**

217 The top classified taxa obtained from NGS and Nanopore datasets were compared with those
218 inferred by Sanger *I6S* using built-in programs and BLAST+ for analysis. Species-level
219 concordance between the HTS and Sanger workflows was calculated. For samples that did not
220 match at the species level, concordance at the genus or family level was determined.

221 To assess diagnostic accuracy, a composite *16S* rRNA sequencing result of the three sequencing
222 platforms was considered as the reference standard. Identical species obtained by at least two
223 sequencing platforms were considered as reference taxa. For samples with complete discordant
224 species inferred by the three sequencing platforms, WGS was conducted to confirm the reference
225 taxa.

226

227

228 RESULTS

229 **Statistics of sequencing reads generated from the NGS and Nanopore workflows**

230 Based on the default analysis of MSR, the NGS platform generated an average of 113,381 reads
231 per sample. After merging the paired-end reads and filtering out unwanted reads with undesired
232 read lengths and ambiguous bases, an average of 68,652 filtered reads per sample was retained
233 for NGS_BLAST+ analysis.

234 The Nanopore MinKNOW platform generated an average of 51,769 reads ($QSCORE \geq 7$) per
235 sample, but an average of 51,419 reads ($QSCORE \geq 7$) per sample was analyzed in the FASTQ
236 16S workflow in Epi2me. The slight difference in the number of average reads per sample was
237 due to using different algorithms in the demultiplexing step between Epi2me and Guppy
238 (MinKNOW). An average of 51,769 reads per sample was analyzed using NanoBLAST+.

239 The total number of reads and the number of classified reads of each sample on both sequencing
240 platforms are shown in Table S3.

241

242 **Taxonomic resolution of sequencing reads**

243 The percentage distribution of classified reads via both sequencing platforms is shown in Figure
244 1. On average, only 45.74% of the total reads of a sample were successfully classified at the
245 species level by MSR with reference to the Greengenes database. After merging paired-end reads
246 and quality filtering, 94.02% of filtered reads were classified at the species level by
247 NGS_BLAST+ with reference to the NCBI *16S* rRNA database.

248 In the Nanopore workflow, both Epi2me and NanoBLAST+ use the NCBI *16S* rRNA database
249 for classification of long-read sequencing data. An average of 76.03% of total reads were
250 classified at the species level in Epi2me, compared with 53.56% in NanoBLAST+.

251

252 **Concordance in bacterial speciation by Sanger, Illumina and Nanopore *16S* rRNA** 253 **sequencing**

254 The top-ranked species obtained from the NGS *16S* and Nanopore *16S* workflows, coupled with
255 the respective analysis pipelines, are listed in Table S3 The percentage of samples that matched
256 with Sanger *16S* at each of the species, genus and family levels is illustrated in Figure 2. The
257 concordance in species-level identification among the sequencing platforms is shown in Figure
258 3. Overall, in terms of concordance with the Sanger *16S* result, Nanopore *16S* was better than
259 NGS *16S* (154/172 [89.53%] vs. 113/172 [65.70%], respectively), regardless of analysis
260 pipeline.

261 For the NGS *16S* workflow, MSR and NGS_BLAST+ demonstrated a concordance of 33.14%
262 (57/172) and 65.70% (113/172), respectively, with Sanger *16S* in species-level identification. A
263 total of 9.30% of samples (16/172) were unmatched, even at the family level, in MSR, whereas
264 all samples matched at the family level or below in NGS_BLAST+. Of note, concordance
265 between the results of MSR and NGS_BLAST+ was low; only 32.56% of samples (56/172)
266 showed a matched result among the classified species from these two analysis pipelines.
267 Moreover, only 28.49% of samples (49/172) showed complete agreement in the classified
268 species among the MSR, NGS_BLAST+, and Sanger datasets. Owing to poor concordance of
269 the MSR analysis with other sequencing methods, NGS_BLAST+ was considered as the optimal

270 analysis method for the Illumina datasets, and its results were regarded as the final identification
271 inferred by the NGS *16S* workflow.

272 For Nanopore *16S*, a concordance of 87.79% (151/172) and 83.14% (143/172) at the species
273 level was achieved with Epi2me and NanoBLAST+, respectively. A total of 1.16% of samples
274 (2/172) were unmatched, as reported by Epi2me and NanoBLAST+, respectively. Concordance
275 between the results of Epi2me and NanoBLAST+ was 80.23% (138/172). Additionally, 76.74%
276 of samples (132/172) showed agreement in the classified species among the Epi2me,
277 NanoBLAST+ and Sanger datasets.

278 A total of 34 samples showed disagreement in the classified species inferred by Epi2me and
279 NanoBLAST+. The respective Nanopore data were further analyzed using NanoCLUST to
280 resolve the discrepancies. NanoCLUST agreed with Epi2ME and BLAST+ in 13 (38.24%) and
281 17 (50.00%) samples, respectively. Four samples failed to reach agreement in terms of species-
282 level identification, in which three were matched in terms of genus-level identification, and one
283 was considered as having no reliable bacterial ID. Concordance between the resolved Nanopore
284 *16S* and Sanger *16S* was 89.53% (154/172).

285

286 **WGS for bacterial isolates with discrepant species-level ID**

287 Eight samples (4.65% [8/172]) showed complete discordance in bacterial species, as inferred by
288 the three *16S* rRNA sequencing workflows. WGS was conducted to identify definite taxa.
289 Interestingly, seven of these samples failed to match with the published bacterial genomes, with
290 query coverage of <70% for the longest consensus sequences (Table 1). The ANIs to the best-
291 matched genomes were <85% (Threshold for the same species should be >94%) , suggesting that

292 these seven “difficult-to-identify” isolates were likely novel bacterial species. As the definite
293 bacterial species could not be confirmed, these samples were excluded from the subsequent
294 diagnostic evaluation.

295 The consensus sequence of one sample (R062) showed an overall query coverage of >92%, with
296 99.17% identity to *Klebsiella michiganensis* (NZ_CP060111.1). As the ANI achieved 98.71%,
297 *K. michiganensis* was therefore considered as the reference taxon for this sample.

298

299 **Diagnostic accuracy of the three 16S rRNA sequencing workflows**

300 Considering the composite of 16S rRNA sequencing and WGS results as reference standards, the
301 diagnostic accuracy of Sanger 16S, NGS 16S and Nanopore 16S was 96.36% (159/165), 71.52%
302 (118/165) and 96.36% (159/165), respectively, for species-level identification of “difficult-to-
303 identify” bacterial pathogens (Figure 3). The mismatched samples in at least one of the
304 sequencing methods were listed in Table 2. The diagnostic performance of each sequencing
305 workflow was summarized in Table 3.

306

307 **Comparison of sample-to-report time and running cost of the two HTS technologies**

308 The Illumina platform enables sequencing of up to 384 samples per run, whereas, owing to the
309 limited choice of sequencing barcodes, the Nanopore platform can only support a batch of 24
310 samples per run. Without considering the time for DNA extraction, it took 78 h for the Illumina
311 workflow to generate sequencing data for each run (Figure 4). With the Nanopore platform, the
312 sequencing workflow required 8.25 h. Of note, although base-calling and Epi2me analyses are

313 real-time processes, their speed is highly dependent on the strength of the computer. However,
314 Nanopore sequencing can be stopped once sufficient reads have been generated.

315 The running cost of the Nanopore workflow is relatively lower than that of the Illumina
316 workflow. The cost of the Illumina workflow per sequencing run is US \$4,931 (172 samples),
317 and the cost per sample is approximately US \$28.7. If the sample size is increased to 384, the
318 cost of the Illumina workflow per sequencing run is US \$8,279; therefore, the cost per sample is
319 reduced to US \$21.6. For the Nanopore workflow, the cost per sequencing run (24 samples) is
320 US \$424, which means that the cost per sample is approximately US \$17.7.

321

322 DISCUSSION

323 Although the majority of bacterial pathogens can be identified by MALDI-TOF MS, *16S* rRNA
324 gene sequencing is needed in clinical microbiology laboratories to confirm the identities of
325 “difficult-to-identify” clinical isolates. With reduced costs, simplified protocols and automated
326 bioinformatics pipelines, HTS has been proposed as a better alternative to Sanger sequencing for
327 sequence-based bacterial identification in clinical laboratories. This is the first study to compare
328 the performance (and evaluate the clinical utility) of two commercially available high-throughput
329 *16S* rRNA gene sequencing assays with built-in analysis software for taxonomic assignment of
330 bacterial pathogens that are unidentifiable using MALDI-TOF MS.

331 With the Illumina platform, the concordance of the classified species between MSR and Sanger
332 *16S* was exceptionally low; only 33.14% of samples matched the reference at top classified
333 species compared with 65.70% when using NGS_BLAST+. As described in previous studies, the
334 use of different bioinformatic tools and *16S* rRNA sequence databases could result in different
335 taxonomic assignments, especially at lower taxonomic levels (24, 25). The latest version of the
336 Greengenes database for MSR was updated in 2013 and does not contain certain new bacterial
337 taxa, which accounts for the poor agreement of this workflow compared with others (25).

338 Nevertheless, mismatches between NGS and Sanger sequencing were observed in 34.33% of
339 samples, even when the same aligner (i.e., BLAST+) and database (i.e., NCBI 16S bacterial
340 database) were used. One may argue that, with the constraint of low sequencing depth, the
341 Sanger *16S* result alone should not be considered as the final reference. We used a composite of
342 *16S* sequencing results generated by three platforms, and any discrepancies were resolved by
343 WGS as the reference standard to determine the diagnostic accuracy of the HTS workflows.
344 Eventually, a total of 47 samples, including 29 genera and 37 species (Table S3), remained

345 discordant between NGS *16S* and the reference standard. As indicated by Johnson *et al.*,
346 although some sub-regions (e.g., V1–V3) of *16S* s rRNA gene provide a reasonable
347 approximation of *16S* diversity, most do not capture sufficient sequence variation to discriminate
348 between closely related taxa. Also, different sub-regions show bias in the bacterial taxa that can
349 be identified (26). In this study, V3–V4 regions might perform poorly in classifying the genera
350 of discordant samples.

351 Availability of third-generation technologies means that it is becoming possible to exploit the
352 full discriminatory potential of the entire *16S* rRNA gene in a high-throughput manner. The
353 Nanopore *16S* workflow demonstrated a considerably higher percentage concordance with the
354 Sanger *16S* workflow compared with the NGS *16S* workflow, regardless of the analysis pipeline
355 used. In contrast to the built-in analysis on the Illumina platform (i.e., MSR), the performance of
356 Epi2me with Nanopore *16S* was comparable to that of nanoBLAST+ (83.14%), with 87.79% of
357 samples matching Sanger *16S* at top classified species.

358 Notably, species-level disagreement between Epi2me and nanoBLAST+ was observed in 34
359 samples (19.77%) and was subsequently resolved by NanoCLUST. Epi2me and BLAST+ rely
360 on read-by-read alignment to reference sequences in the database. As the base-calling accuracy
361 of Nanopore sequencing is relatively low, the prevalence of sequencing errors in Nanopore reads
362 could limit its ability to resolve highly similar sequences. Alternatively, NanoCLUST generates
363 clusters based on Uniform Manifold Approximation and Projection and classifies the
364 representative consensus read in each cluster using BLAST. The effect of sequencing errors in
365 individual sequences can be minimized by forming clusters, which reduces the chance of
366 misclassification. Comparing the species resolved using NanoCLUST with the reference

367 standard, there was a slight improvement in diagnostic accuracy from 89.09% (Epi2me) and
368 89.70% (nanoBLAST+) to 96.36%.

369 Six samples (3.64%) failed to match the reference at the species level in the optimized Nanopore
370 *16S* workflow. One possible reason for this discordance is the high similarity in *16S* rRNA gene
371 sequences between the inferred species and the reference taxa. Based on the now historic
372 assumption of *16S* rRNA sequencing, sequences with >95% identity represent the same genus,
373 whereas sequences with >97% identity represent closely related species (27). Many researchers
374 have reported that the taxonomic resolution of *16S* rRNA gene is lower and is unable to
375 discriminate the closely related species in certain genera, including but not limited to *Bacillus*,
376 *Burkholderia*, *Acinetobacter baumannii-calcoaceticus complex*, *Achromobacter*, *Actinomyces*
377 and *Staphylococcus* and the Enterobacteriaceae family (28, 29). In this study, all six taxa inferred
378 by Nanopore *16S* had >97% sequence identity with the reference standard (Table 2).

379 In this study, WGS was performed to identify the definite bacterial taxa for samples with
380 completely discordant *16S* results. To validate the transposase-based rapid sequencing protocol
381 for bacterial genome construction, two reference strains, namely *Klebsiella pneumoniae*
382 BAA3079 and *Staphylococcus aureus* BAA3114, were sequenced and analyzed in parallel with
383 the eight discordant samples. Both strains successfully yielded consensus sequences of >3Mb,
384 which covered 94% of the genomes of the respective target organisms with 99% identity. This
385 indicated that the WGS protocol was able to construct reliable consensus prokaryotic genomes
386 (Table 1). Nonetheless, the longest consensus sequences of the seven discordant samples failed
387 to obtain a query coverage >50% when mapped to the NCBI Prokaryotic RefSeq Genomes
388 database, suggesting no significant matches between these samples and published bacterial
389 genomes. The ANIs to the best-matched genomes were <94%. These “difficult-to-identify”

390 isolates were therefore considered as novel bacterial species (30). WGS confirmed that R062
391 belonged to *K. michiganensis* (ANI = 98.71%), which shared a high degree of *16S* rRNA identity
392 with the taxa assigned by Sanger *16S* (*Klebsiella grimontii*; 99.20%), NGS *16S* (*Enterobacter*
393 *cloacae*; 97.07%) and Nanopore *16S* (*Yokenella regensburgei*; 98.56%) (Table 1). This explains
394 why *16S* rRNA sequencing was not able to accurately differentiate these species.

395 Considering the time-to-result of the two sequencing platforms, the Nanopore workflow has a
396 much shorter turnaround time compared with the Illumina workflow (8.25 h and 78 h,
397 respectively). Therefore, faster results can be obtained with the Nanopore workflow. However,
398 the sample size is limited to 24 samples per batch. Comparing the cost per sample in a
399 sequencing run, Nanopore sequencing is relatively cheaper than Illumina sequencing (US \$17.7
400 vs. US \$28.6, respectively). Additionally, the startup cost of Nanopore sequencing is remarkably
401 lower than that of Illumina sequencing. The starter package of Nanopore sequencing costs only
402 US \$1,000, whereas Illumina MiSeq costs approximately US \$125,000.

403 The reusable flow cell FLO-MIN106 R9.4.1, which enables sequencing for up to 72 h, was used
404 for Nanopore 16S in this study. However, library carry over from previous run was observed in a
405 pilot study. This is problematic when the same barcode set is used in consecutive sequencing
406 run. To avoid contamination by library carry over, a new flow cell was used in each sequencing
407 run, and used flow cells were reserved for other sequencing runs using different barcodes. In this
408 context, the disposable Flongle flow cell from ONT is more suitable in a clinical setting. The
409 Flongle flow cell, which costs only US \$90, can sequence for up to 16 h. Although the number of
410 active pores available in the Flongle flow cell is lower, it is more cost- and time-effective when
411 the sample size is small. Since it takes time to accumulate a batch of 24 “difficult-to-identify”

412 isolates in clinical laboratories, a small sample size per sequencing run will be beneficial,
413 especially for cases that require urgent diagnosis.

414 There are some limitations in this study that should be noted. First, the aim of this study was to
415 compare commercially available kits for *16S* rRNA gene sequencing from Illumina and
416 Nanopore. Therefore, by using the 16S Metagenomic Sequencing Library Preparation kit, only
417 the V3–V4 sub-regions of *16S* rRNA gene were sequenced in the Illumina workflow. But it is
418 possible to sequence full-length *16S* rRNA gene using Illumina MiSeq with a laboratory
419 developed protocol(31), which may increase the taxonomic resolution of the Illumina workflow
420 at the species level. Second, except for the eight discordant samples, the reference taxa of
421 isolates were defined by *16S* rRNA sequencing without being confirmed by WGS. However,
422 some closely related species may have identical *16S* rRNA genes; thus, *16S* rRNA sequencing
423 results may not represent the definite taxa of these samples. Third, regarding the eight samples
424 that underwent WGS, the taxonomic assignment was based on the contigs of consensus
425 sequences after de novo assembly. Circular, gap-free bacterial genomes were not constructed.
426 Finally, bacterial DNA for *16S* sequencing was extracted from cultured isolates. The
427 performance of the NGS *16S* and Nanopore *16S* workflows on direct bacterial identification in
428 microbial and polymicrobial specimens was not evaluated.

429

430 **CONCLUSION**

431 In conclusion, the commercial *16S* rRNA gene sequencing workflow from ONT (SQK-16S024),
432 coupled with NanoCLUST, is the most accurate for bacterial identification in a clinical setting,

433 with higher flexibility in sample size and sequencing time, a lower running cost, and higher
434 concordance with the reference standard.

435

436 **ACKNOWLEDGMENTS**

437 This work was supported by the Innovation and Technology Fund - Partnership Research
438 Programme (PRP) (PRP/010/20FX). The funders had no role in study design, data collection and
439 interpretation, or the decision to submit the work for publication.

440 **DECLARATION OF INTEREST STATEMENT**

441 We declare no competing interests.

442

443 **REFERENCES**

- 444 1. Jesumirhewe C, Ogunlowo PO, Olley M, Springer B, Allerberger F, Ruppitsch W. 2016.
445 Accuracy of conventional identification methods used for Enterobacteriaceae isolates in
446 three Nigerian hospitals. *PeerJ* 4:e2511.
- 447 2. Harmsen D, Rothganger J, Frosch M, Albert J. 2002. RIDOM: Ribosomal Differentiation
448 of Medical Micro-organisms Database. *Nucleic Acids Res* 30:416-7.
- 449 3. Karger A. 2016. Current developments to use linear MALDI-TOF spectra for the
450 identification and typing of bacteria and the characterization of other cells/organisms
451 related to infectious diseases. *Proteomics Clin Appl* 10:982-993.
- 452 4. Patel R. 2015. MALDI-TOF MS for the diagnosis of infectious diseases. *Clin Chem*
453 61:100-11.
- 454 5. Hou TY, Chiang-Ni C, Teng SH. 2019. Current status of MALDI-TOF mass
455 spectrometry in clinical microbiology. *J Food Drug Anal* 27:404-414.
- 456 6. Lau SK, Tang BS, Teng JL, Chan TM, Curreem SO, Fan RY, Ng RH, Chan JF, Yuen
457 KY, Woo PC. 2014. Matrix-assisted laser desorption ionisation time-of-flight mass
458 spectrometry for identification of clinically significant bacteria that are difficult to
459 identify in clinical laboratories. *J Clin Pathol* 67:361-6.
- 460 7. Ge MC, Kuo AJ, Liu KL, Wen YH, Chia JH, Chang PY, Lee MH, Wu TL, Chang SC, Lu
461 JJ. 2017. Routine identification of microorganisms by matrix-assisted laser desorption
462 ionization time-of-flight mass spectrometry: Success rate, economic analysis, and clinical
463 outcome. *J Microbiol Immunol Infect* 50:662-668.
- 464 8. Garner O, Mochon A, Branda J, Burnham CA, Bythrow M, Ferraro M, Ginocchio C,
465 Jennemann R, Manji R, Procop GW, Richter S, Rychert J, Sercia L, Westblade L,

- 466 Lewinski M. 2014. Multi-centre evaluation of mass spectrometric identification of
467 anaerobic bacteria using the VITEK(R) MS system. *Clin Microbiol Infect* 20:335-9.
- 468 9. Knoester M, van Veen SQ, Claas EC, Kuijper EJ. 2012. Routine identification of clinical
469 isolates of anaerobic bacteria: matrix-assisted laser desorption ionization-time of flight
470 mass spectrometry performs better than conventional identification methods. *J Clin*
471 *Microbiol* 50:1504.
- 472 10. Luo Y, Siu GKH, Yeung ASF, Chen JHK, Ho PL, Leung KW, Tsang JLY, Cheng VCC,
473 Guo L, Yang J, Ye L, Yam WC. 2015. Performance of the VITEK MS matrix-assisted
474 laser desorption ionization-time of flight mass spectrometry system for rapid bacterial
475 identification in two diagnostic centres in China. *J Med Microbiol* 64:18-24.
- 476 11. Bizzini A, Jaton K, Romo D, Bille J, Prod'homme G, Greub G. 2011. Matrix-assisted laser
477 desorption ionization-time of flight mass spectrometry as an alternative to 16S rRNA
478 gene sequencing for identification of difficult-to-identify bacterial strains. *J Clin*
479 *Microbiol* 49:693-6.
- 480 12. Homem de Mello de Souza HAP, Dalla-Costa LM, Vicenzi FJ, Camargo de Souza D,
481 Riedi CA, Filho NAR, Pilonetto M. 2014. MALDI-TOF: a useful tool for laboratory
482 identification of uncommon glucose non-fermenting Gram-negative bacteria associated
483 with cystic fibrosis. *J Med Microbiol* 63:1148-1153.
- 484 13. Winand R, Bogaerts B, Hoffman S, Lefevre L, Delvoeye M, Braekel JV, Fu Q, Roosens
485 NH, Keersmaecker SC, Vanneste K. 2019. Targeting the 16s Rrna Gene for Bacterial
486 Identification in Complex Mixed Samples: Comparative Evaluation of Second (Illumina)
487 and Third (Oxford Nanopore Technologies) Generation Sequencing Technologies. *Int J*
488 *Mol Sci* 21.
- 489 14. Chakravorty S, Helb D, Burday M, Connell N, Alland D. 2007. A detailed analysis of
490 16S ribosomal RNA gene segments for the diagnosis of pathogenic bacteria. *J Microbiol*
491 *Methods* 69:330-9.
- 492 15. Ip CLC, Loose M, Tyson JR, de Cesare M, Brown BL, Jain M, Leggett RM, Eccles DA,
493 Zalunin V, Urban JM, Piazza P, Bowden RJ, Paten B, Mwaigwisya S, Batty EM,
494 Simpson JT, Snutch TP, Birney E, Buck D, Goodwin S, Jansen HJ, O'Grady J, Olsen HE,
495 Min IONA, Reference C. 2015. MinION Analysis and Reference Consortium: Phase 1
496 data release and analysis. *F1000Res* 4:1075.
- 497 16. Muyzer G, Teske A, Wirsén CO, Jannasch HW. 1995. Phylogenetic relationships of
498 *Thiomicrospira* species and their identification in deep-sea hydrothermal vent samples by
499 denaturing gradient gel electrophoresis of 16S rDNA fragments. *Arch Microbiol*
500 164:165-72.
- 501 17. Liu Z, Lozupone C, Hamady M, Bushman FD, Knight R. 2007. Short pyrosequencing
502 reads suffice for accurate microbial community analysis. *Nucleic Acids Res* 35:e120.
- 503 18. Andersson AF, Lindberg M, Jakobsson H, Backhed F, Nyren P, Engstrand L. 2008.
504 Comparative analysis of human gut microbiota by barcoded pyrosequencing. *PLoS One*
505 3:e2836.
- 506 19. Nossa CW, Oberdorf WE, Yang L, Aas JA, Paster BJ, Desantis TZ, Brodie EL, Malamud
507 D, Poles MA, Pei Z. 2010. Design of 16S rRNA gene primers for 454 pyrosequencing of
508 the human foregut microbiome. *World J Gastroenterol* 16:4135-44.
- 509 20. Schloss PD, Westcott SL, Ryabin T, Hall JR, Hartmann M, Hollister EB, Lesniewski RA,
510 Oakley BB, Parks DH, Robinson CJ, Sahl JW, Stres B, Thallinger GG, Van Horn DJ,
511 Weber CF. 2009. Introducing mothur: open-source, platform-independent, community-

- 512 supported software for describing and comparing microbial communities. *Appl Environ*
513 *Microbiol* 75:7537-41.
- 514 21. Rodriguez-Perez H, Ciuffreda L, Flores C. 2020. NanoCLUST: a species-level analysis
515 of 16S rRNA nanopore sequencing data. *Bioinformatics*
516 doi:10.1093/bioinformatics/btaa900.
- 517 22. Huang YT, Liu PY, Shih PW. 2021. Homopolish: a method for the removal of systematic
518 errors in nanopore sequencing by homologous polishing. *Genome Biol* 22:95.
- 519 23. Yoon SH, Ha SM, Lim J, Kwon S, Chun J. 2017. A large-scale evaluation of algorithms
520 to calculate average nucleotide identity. *Antonie Van Leeuwenhoek* 110:1281-1286.
- 521 24. Sierra MA, Li Q, Pushalkar S, Paul B, Sandoval TA, Kamer AR, Corby P, Guo Y, Ruff
522 RR, Alekseyenko AV, Li X, Saxena D. 2020. The Influences of Bioinformatics Tools and
523 Reference Databases in Analyzing the Human Oral Microbial Community. *Genes (Basel)*
524 11.
- 525 25. Park SC, Won S. 2018. Evaluation of 16S rRNA Databases for Taxonomic Assignments
526 Using Mock Community. *Genomics Inform* 16:e24.
- 527 26. Johnson JS, Spakowicz DJ, Hong BY, Petersen LM, Demkowicz P, Chen L, Leopold SR,
528 Hanson BM, Agresta HO, Gerstein M, Sodergren E, Weinstock GM. 2019. Evaluation of
529 16S rRNA gene sequencing for species and strain-level microbiome analysis. *Nat*
530 *Commun* 10:5029.
- 531 27. Schloss PD, Handelsman J. 2005. Introducing DOTUR, a computer program for defining
532 operational taxonomic units and estimating species richness. *Appl Environ Microbiol*
533 71:1501-6.
- 534 28. Janda JM, Abbott SL. 2007. 16S rRNA gene sequencing for bacterial identification in the
535 diagnostic laboratory: pluses, perils, and pitfalls. *J Clin Microbiol* 45:2761-4.
- 536 29. Church DL, Cerutti L, Gurtler A, Griener T, Zelazny A, Emler S. 2020. Performance and
537 Application of 16S rRNA Gene Cycle Sequencing for Routine Identification of Bacteria
538 in the Clinical Microbiology Laboratory. *Clin Microbiol Rev* 33.
- 539 30. Konstantinidis KT, Tiedje JM. 2005. Genomic insights that advance the species
540 definition for prokaryotes. *Proc Natl Acad Sci U S A* 102:2567-72.

541

542

Table 1: Whole genome sequencing analysis for the samples with complete discordant taxonomic assignment by Sanger, NGS and Nanopore 16s rRNA sequencing

Sample ID	Species inferred by Sanger 16s	Species inferred by NGS 16s	Species inferred by Nanopore 16s	Whole genome sequencing (WGS)						
				Best-matched Species by WGS (reference genome)	Genome assembly method					
					Shasta			Miniasm		
					Query coverage (%)	Identity (%)	ANI (%) ^b	Query coverage (%)	Identity (%)	ANI (%) ^b
<i>Klebsiella pneumoniae</i> BAA3079 ^a	<i>Klebsiella pneumoniae</i>	<i>Klebsiella pneumoniae</i>	<i>Klebsiella pneumoniae</i>	<i>Klebsiella pneumoniae</i> (NC_016845.1)	99	97.00	98.92	92.13	99.40	99.14
<i>Staphylococcus aureus</i> BAA3114 ^a	<i>Staphylococcus aureus</i>	<i>Staphylococcus aureus</i>	<i>Staphylococcus aureus</i>	<i>Staphylococcus aureus</i> (NC_007795.1)	94.06	99.95	99.30	88.39	99.92	99.23
R001	<i>Kocuria koreensis</i>	<i>Kocuria massiliensis</i>	<i>Kocuria spp.</i>	<i>Kocuria massiliensis</i> (NZ_LT835161.1)	42.21	87.44	78.29	42.42	87.41	78.55
R006	<i>Kocuria koreensis</i>	<i>Kocuria massiliensis</i>	<i>Kocuria spp.</i>	<i>Kocuria massiliensis</i> (NZ_LT835161.1)	43.04	79.12	78.49	42.04	87.49	78.44
R062	<i>Klebsiella grimontii</i>	<i>Enterobacter cloacae</i>	<i>Yokenella regensburgei</i>	<i>Klebsiella michiganensis</i> (NZ_CP060111.1)	92.17	99.17	98.71	86.30	98.99	98.69
R120	<i>Brachybacterium conglomeratum</i>	<i>Brachybacterium faecium</i>	<i>Brachybacterium paraconglomeratum</i>	<i>Brachybacterium saurashtrense</i> (NZ_CP031356.1)	62.15	85.18	82.30	62.30	85.12	82.39
R121	<i>Schaalia odontolytica</i>	<i>Schaalia vaccimaxillae</i>	<i>Sphingomonas paucimobilis</i>	<i>Schaalia odontolytica</i> (NZ_CP046315.1)	6.07	78.55	70.34	6.04	78.24	70.86
R131	<i>Schaalia odontolytica</i>	<i>Schaalia vaccimaxillae</i>	No reliable ID	<i>Schaalia odontolytica</i> (NZ_CP046315.1)	6.19	82.12	71.21	6.29	78.25	71.26
R158	<i>Microbacterium ginsengite rrae</i>	<i>Microbacterium assamensis</i>	<i>Microbacterium foliorum</i>	<i>Microbacterium foliorum</i> (NZ_CP041040.1)	65.41	84.52	82.24	65.21	84.51	82.15
R181	<i>Sphingomonas yabuuchi ae</i>	<i>Sphingomonas paucimobilis</i>	<i>Sphingomonas sanguinis</i>	<i>Sphingomonas hominis</i> (NZ_JABULH010000007.1)	31.48	89.67	82.09	30.68	89.59	81.95

^a *Klebsiella pneumoniae* BAA3079 and *Staphylococcus aureus* BAA3114 served as QC sample, which were sequenced and analyzed in parallel with the discordant samples for WGS and bioinformatics analysis.

^b Average Nucleotide Identity (ANI) > 94% indicated that the samples belong to the same species as the best-matched genomes.

Table 2: The samples with mismatched taxa inferred by at least one sequencing platform

Sample ID	Species-level ID (Reference Standard)	Sanger Sequencing (Sanger 16s)		Illumina Sequencing (NGS 16s)		Nanopore Sequencing (Nanopore 16s)	
		Classified species from Sanger 16s ^a	16s Identity against the reference (%)	Classified species from NGS 16s ^a	16s Identity against the reference (%)	Classified species from Nanopore 16s ^a	16s Identity against the reference (%)
R003	<i>Pseudoglutamicibacter albus</i>	<u><i>Pseudoglutamicibacter cumminsii</i></u>	99.26%	<i>Pseudoglutamicibacter albus</i>	matched	<i>Pseudoglutamicibacter albus</i>	matched
R013	<i>Microbacterium hominis</i>	<i>Microbacterium hominis</i>	matched	<u><i>Microbacterium aerolatum</i></u>	97.47%	<i>Microbacterium hominis</i>	matched
R017	<i>Microbacterium hominis</i>	<i>Microbacterium hominis</i>	matched	<u><i>Microbacterium aerolatum</i></u>	97.47%	<i>Microbacterium hominis</i>	matched
R021	<i>Microbacterium hominis</i>	<i>Microbacterium hominis</i>	matched	<u><i>Microbacterium aerolatum</i></u>	97.47%	<i>Microbacterium hominis</i>	matched
R024	<i>Bacillus idriensis</i>	<i>Bacillus idriensis</i>	matched	<i>Bacillus idriensis</i>	matched	<u><i>Bacillus indicus</i></u>	97.62%
R025	<i>Varibaculum cambriense</i>	<i>Varibaculum cambriense</i>	matched	<u><i>Varibaculum anthropi</i></u>	98.50%	<i>Varibaculum cambriense</i>	matched
R026	<i>Varibaculum cambriense</i>	<i>Varibaculum cambriense</i>	matched	<u><i>Varibaculum anthropi</i></u>	98.50%	<i>Varibaculum cambriense</i>	matched
R036	<i>Corynebacterium lowii</i>	<i>Corynebacterium lowii</i>	matched	<u><i>Corynebacterium bovis</i></u>	93.29%	<i>Corynebacterium lowii</i>	matched
R040	<i>Weissella cibaria</i>	<i>Weissella cibaria</i>	matched	<u><i>Weissella confusa</i></u>	99.26%	<i>Weissella cibaria</i>	matched
R043	<i>Proteus vulgaris</i>	<i>Proteus vulgaris</i>	matched	<u><i>Proteus alimentorum</i></u>	99.64%	<i>Proteus vulgaris</i>	matched
R045	<i>Brucella microti</i>	<i>Brucella microti</i>	matched	<u><i>Brucella papionis</i></u>	99.86%	<i>Brucella microti</i>	matched
R047	<i>Proteus cibarius</i>	<i>Proteus cibarius</i>	matched	<u><i>Proteus terrae</i></u>	99.65%	<i>Proteus cibarius</i>	matched
R049	<i>Dermacoccus barathri</i>	<i>Dermacoccus barathri</i>	matched	<u><i>Dermacoccus profundi</i></u>	99.86%	<i>Dermacoccus barathri</i>	matched
R052	<i>Arcanobacterium wilhelmae</i>	<i>Arcanobacterium wilhelmae</i>	matched	<u><i>Arcanobacterium pinnipediorum</i></u>	96.60%	<i>Arcanobacterium wilhelmae</i>	matched
R053	<i>Dermacoccus barathri</i>	<i>Dermacoccus barathri</i>	matched	<u><i>Dermacoccus profundi</i></u>	99.86%	<i>Dermacoccus barathri</i>	matched
R056	<i>Corynebacterium simulans</i>	<i>Corynebacterium simulans</i>	matched	<u><i>Corynebacterium glutamicum</i></u>	93.74%	<i>Corynebacterium simulans</i>	matched
R058	<i>Corynebacterium mastitidis</i>	<i>Corynebacterium mastitidis</i>	matched	<u><i>Corynebacterium tuberculostearicum</i></u>	94.67%	<i>Corynebacterium mastitidis</i>	matched
R062	<i>Klebsiella michiganensis</i>	<u><i>Klebsiella grimonii</i></u>	99.20%	<u><i>Enterobacter cloacae</i></u>	97.07%	<u><i>Yokenella regensburgei</i></u>	98.56%
R063	<i>Corynebacterium pilbarensis</i>	<i>Corynebacterium pilbarensis</i>	matched	<u><i>Corynebacterium coyleae</i></u>	98.04%	<i>Corynebacterium pilbarensis</i>	matched
R069	<i>Eikenella corrodens</i>	<i>Eikenella corrodens</i>	matched	<u><i>Eikenella halliae</i></u>	98.69%	<i>Eikenella corrodens</i>	matched
R071	<i>Corynebacterium xerosis</i>	<u><i>Corynebacterium hansenii</i></u>	99.07%	<i>Corynebacterium xerosis</i>	matched	<i>Corynebacterium xerosis</i>	matched
R072	<i>Mycolicibacterium fortuitum</i>	<i>Mycolicibacterium fortuitum</i>	matched	<u><i>Mycolicibacterium arcueilense</i></u>	98.96%	<i>Mycolicibacterium fortuitum</i>	matched
R073	<i>Tessaracoccus oleiagri</i>	<i>Tessaracoccus oleiagri</i>	matched	<u><i>Tessaracoccus flavescens</i></u>	95.95%	<i>Tessaracoccus oleiagri</i>	matched
R078	<i>Vagococcus teuberi</i>	<i>Vagococcus teuberi</i>	matched	<u><i>Vagococcus martis</i></u>	99.22%	<i>Vagococcus teuberi</i>	matched
R079	<i>Corynebacterium xerosis</i>	<u><i>Corynebacterium hansenii</i></u>	99.07%	<i>Corynebacterium xerosis</i>	matched	<i>Corynebacterium xerosis</i>	matched
R083	<i>Tessaracoccus oleiagri</i>	<i>Tessaracoccus oleiagri</i>	matched	<u><i>Tessaracoccus flavescens</i></u>	95.95%	<i>Tessaracoccus oleiagri</i>	matched
R086	<i>Raoultella planticola</i>	<i>Raoultella planticola</i>	matched	<i>Raoultella planticola</i>	matched	<u><i>Klebsiella aerogenes</i></u>	99.06%
R094	<i>Corynebacterium xerosis</i>	<u><i>Corynebacterium hansenii</i></u>	99.07%	<i>Corynebacterium xerosis</i>	matched	<i>Corynebacterium xerosis</i>	matched

R096	<i>Streptomyces thermodiastaticus</i>	<i>Streptomyces thermodiastaticus</i>	matched	<u><i>Streptomyces thermoviolaceus</i></u>	98.86%	<i>Streptomyces thermodiastaticus</i>	matched
R097	<i>Pseudoxanthomonas helianthi</i>	<i>Pseudoxanthomonas helianthi</i>	matched	<u><i>Pseudoxanthomonas spadix</i></u>	97.04%	<i>Pseudoxanthomonas helianthi</i>	matched
R098	<i>Brachybacterium huguangmaarensis</i>	<i>Brachybacterium huguangmaarensis</i>	matched	<i>Brachybacterium huguangmaarensis</i>	matched	<u><i>Brachybacterium nesterenkovi</i></u>	97.84%
R104	<i>Gordonia sputi</i>	<i>Gordonia sputi</i>	matched	<u><i>Gordonia otitidis</i></u>	99.07%	<i>Gordonia sputi</i>	matched
R105	<i>Gordonia sputi</i>	<i>Gordonia sputi</i>	matched	<u><i>Gordonia otitidis</i></u>	99.07%	<i>Gordonia sputi</i>	matched
R108	<i>Staphylococcus saccharolyticus</i>	<i>Staphylococcus saccharolyticus</i>	matched	<u><i>Staphylococcus epidermidis</i></u>	99.19%	<i>Staphylococcus saccharolyticus</i>	matched
R112	<i>Citrobacter sedlakii</i>	<i>Citrobacter sedlakii</i>	matched	<u><i>Citrobacter youngae</i></u>	98.32%	<i>Citrobacter sedlakii</i>	matched
R116	<i>Tsukamurella tyrosinosolvans</i>	<i>Tsukamurella tyrosinosolvans</i>	matched	<u><i>Tsukamurella ocularis</i></u>	99.86%	<i>Tsukamurella tyrosinosolvans</i>	matched
R123	<i>Pseudoglutamicibacter albus</i>	<u><i>Pseudoglutamicibacter cumminsii</i></u>	99.26%	<i>Pseudoglutamicibacter albus</i>	matched	<i>Pseudoglutamicibacter albus</i>	matched
R133	<i>Nocardia brasiliensis</i>	<i>Nocardia brasiliensis</i>	matched	<u><i>Nocardia vulneris</i></u>	99.31%	<i>Nocardia brasiliensis</i>	matched
R140	<i>Moraxella lacunata</i>	<i>Moraxella lacunata</i>	matched	<u><i>Moraxella equi</i></u>	99.38%	<i>Moraxella lacunata</i>	matched
R141	<i>Ottowia beijingensis</i>	<i>Ottowia beijingensis</i>	matched	<u><i>Brachymonas denitrificans</i></u>	93.33%	<i>Ottowia beijingensis</i>	matched
R149	<i>Ornithinibacillus californiensis</i>	<i>Ornithinibacillus californiensis</i>	matched	<u><i>Ornithinibacillus scapharcae</i></u>	98.48%	<i>Ornithinibacillus californiensis</i>	matched
R151	<i>Dermacoccus barathri</i>	<i>Dermacoccus barathri</i>	matched	<u><i>Dermacoccus profundi</i></u>	99.86%	<i>Dermacoccus barathri</i>	matched
R153	<i>Corynebacterium mastitidis</i>	<i>Corynebacterium mastitidis</i>	matched	<u><i>Corynebacterium tuberculostearicum</i></u>	94.67%	<i>Corynebacterium mastitidis</i>	matched
R175	<i>Corynebacterium pollutisoli</i>	<i>Corynebacterium pollutisoli</i>	matched	<u><i>Corynebacterium humireducens</i></u>	98.07%	<i>Corynebacterium pollutisoli</i>	matched
R176	<i>Tsukamurella ocularis</i>	<i>Tsukamurella ocularis</i>	matched	<i>Tsukamurella ocularis</i>	matched	<u><i>Tsukamurella hominis</i></u>	100.00%
R178	<i>Acinetobacter soli</i>	<i>Acinetobacter soli</i>	matched	<i>Acinetobacter soli</i>	matched	<u><i>Acinetobacter lactucae</i></u>	97.82%
R179	<i>Corynebacterium lipophiloflavum</i>	<i>Corynebacterium lipophiloflavum</i>	matched	<u><i>Corynebacterium mycetoides</i></u>	97.16%	<i>Corynebacterium lipophiloflavum</i>	matched
R180	<i>Corynebacterium mastitidis</i>	<i>Corynebacterium mastitidis</i>	matched	<u><i>Corynebacterium tuberculostearicum</i></u>	94.67%	<i>Corynebacterium mastitidis</i>	matched
R182	<i>Fusobacterium nucleatum</i>	<i>Fusobacterium nucleatum</i>	matched	<u><i>Fusobacterium canifelinum</i></u>	98.34%	<i>Fusobacterium nucleatum</i>	matched
R183	<i>Parabacteroides faecis</i>	<i>Parabacteroides faecis</i>	matched	<u><i>Parabacteroides chongii</i></u>	97.15%	<i>Parabacteroides faecis</i>	matched
R190	<i>Bacillus xiamenensis</i>	<i>Bacillus xiamenensis</i>	matched	<u><i>Bacillus aerius</i></u>	97.16%	<i>Bacillus xiamenensis</i>	matched
R192	<i>Corynebacterium pilbarensis</i>	<i>Corynebacterium pilbarensis</i>	matched	<u><i>Corynebacterium ureicelerivorans</i></u>	98.85%	<i>Corynebacterium pilbarensis</i>	matched
R204	<i>Prevotella scopos</i>	<i>Prevotella scopos</i>	matched	<u><i>Prevotella jejuni</i></u>	97.41%	<i>Prevotella scopos</i>	matched
R205	<i>Pasteurella multocida</i>	<i>Pasteurella multocida</i>	matched	<u><i>Pasteurella stomatis</i></u>	93.74%	<i>Pasteurella multocida</i>	matched
R206	<i>Staphylococcus cohnii</i>	<i>Staphylococcus cohnii</i>	matched	<u><i>Staphylococcus auricularis</i></u>	98.16%	<i>Staphylococcus cohnii</i>	matched
R208	<i>Achromobacter denitrificans</i>	<i>Achromobacter denitrificans</i>	matched	<u><i>Achromobacter xylosoxidans</i></u>	99.15%	<i>Achromobacter denitrificans</i>	matched
R210	<i>Bacillus licheniformis</i>	<i>Bacillus licheniformis</i>	matched	<u><i>Bacillus piscis</i></u>	97.37%	<i>Bacillus licheniformis</i>	matched

Table 3: Diagnostic accuracies of the Sanger, NGS and Nanopore 16s rRNA sequencing methods

Sequencing method	No. of sample analyzed	No. of samples with matched taxa	Diagnostic Accuracy (%)	95% CI
Sanger 16s	165	159	96.36	92.25 - 98.65
Optimized NGS 16s^a	165	118	71.52	63.98 - 78.26
Analyzed by MSR	165	59	35.76	28.46 - 43.58
Analyzed by NGS_BLAST+	165	118	71.52	63.98 - 78.26
Optimized Nanopore 16s^b	165	159	96.36	92.25 - 98.65
Analyzed by Epi2ME	165	147	89.09	83.31 - 93.41
Analyzed by NanoBLAST+	165	148	89.7	84.02 - 93.88

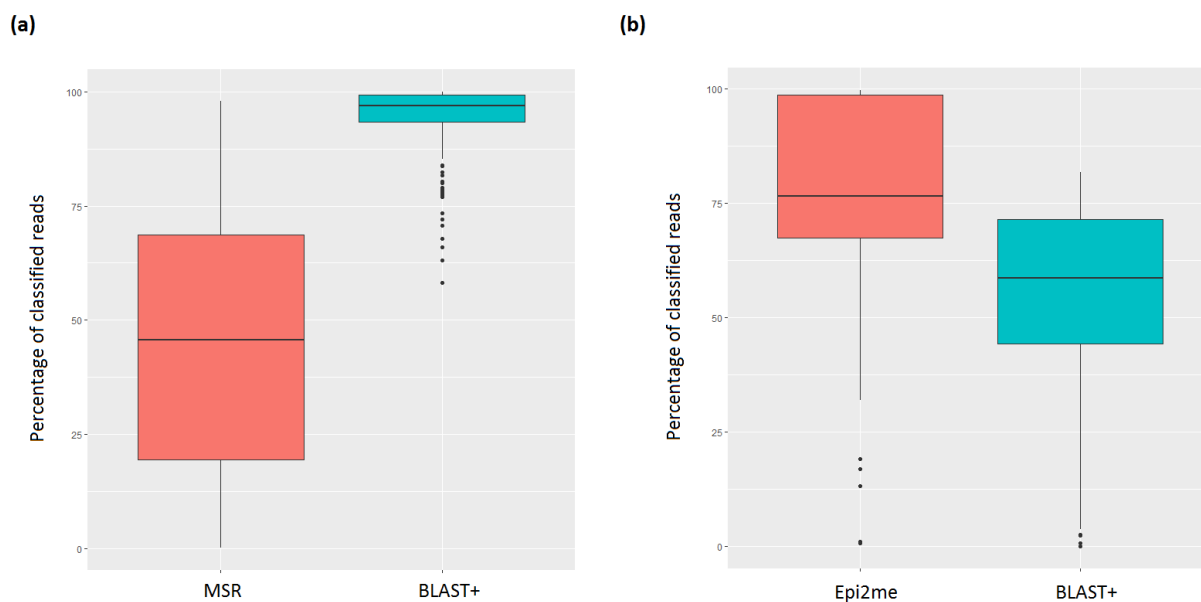
^a Owing to the poor concordance of MSR with other methods, the NGS_BLAST+ was considered as the optimal analysis method for the Illumina datasets

^b The mismatched taxa inferred by Epi2ME and NanoBLAST+ were resolved by NanoCLUST.

545

546

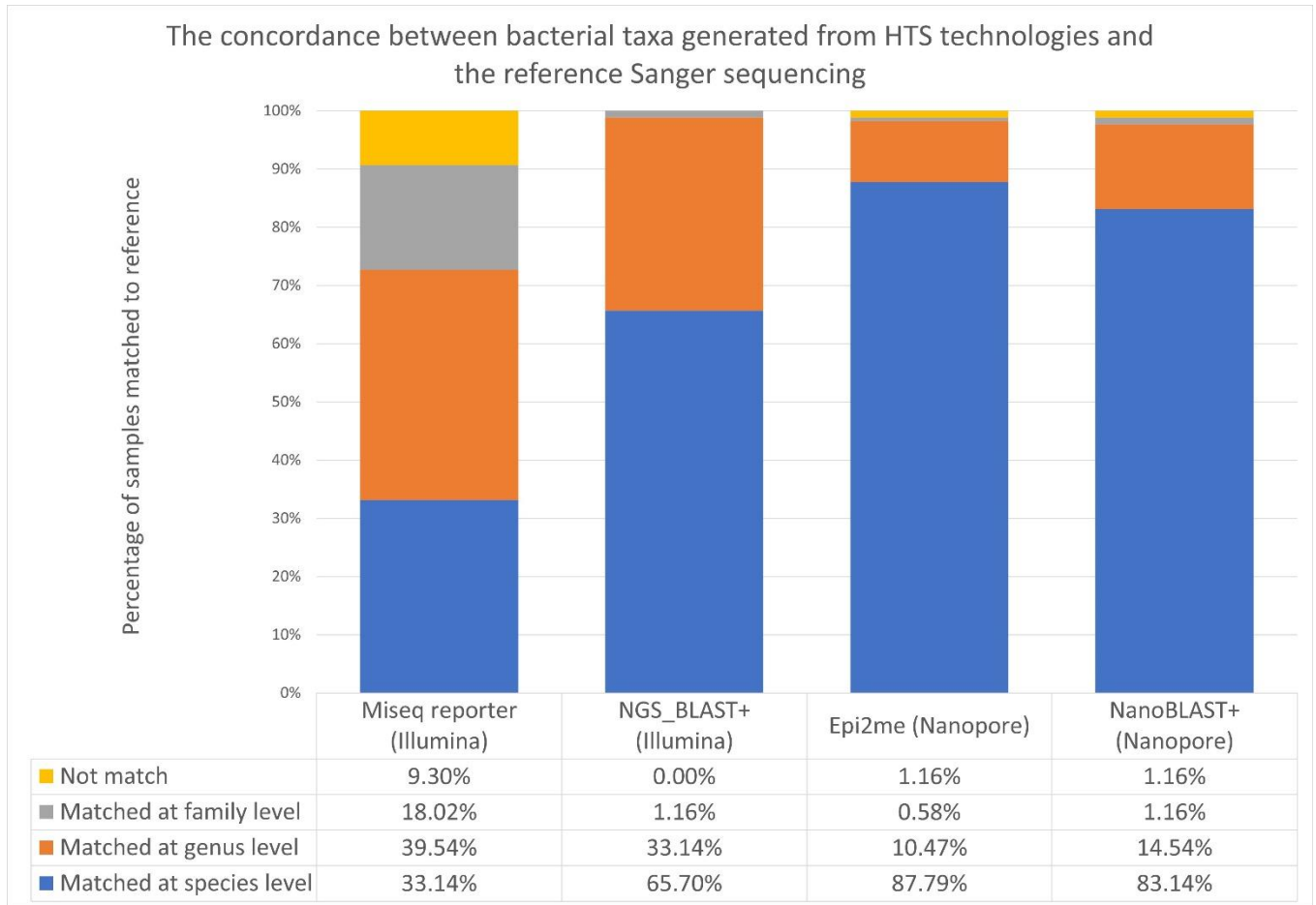
547 **FIGURE LEGENDS**



548

549 Figure 1. The boxplots showing the distribution of percentage of classified reads of all samples in (a)

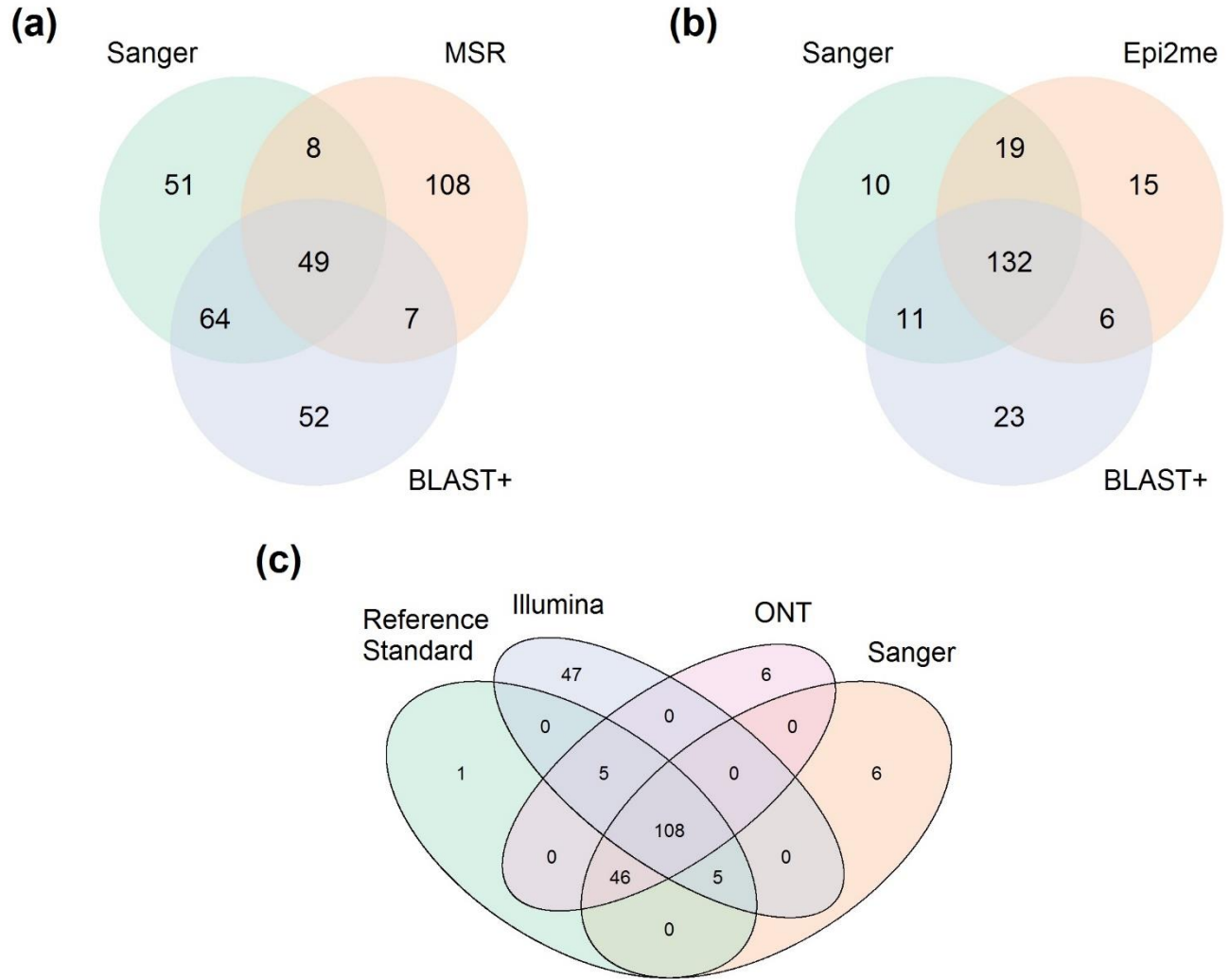
550 Illumina and (b) Nanopore sequencing.



551

552 Figure 2. The concordance between bacterial taxa inferred by the two HTS workflows and the Sanger
 553 sequencing.

554

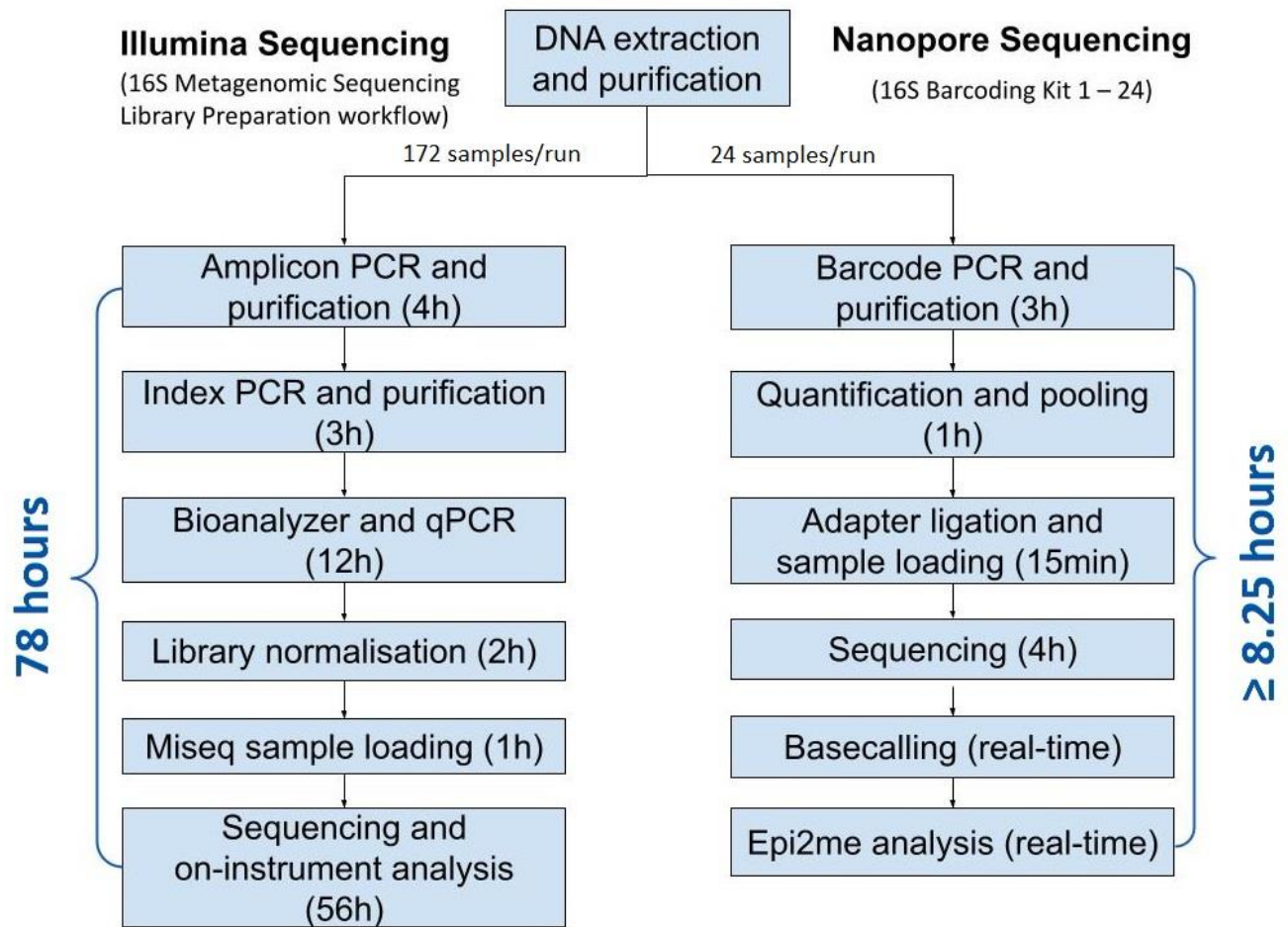


555

556 Figure 3. The Venn Diagram showing the concordance of bacterial taxa inferred by different 16S rRNA
557 sequencing platforms. (a) Concordance of top classified species between Illumina sequencing, coupled
558 with MSR and NGS_BLAST+ analysis, and Sanger sequencing. (b) Concordance of top classified
559 species between Nanopore sequencing, coupled with Epi2ME and nanoBLAST+, and Sanger
560 sequencing. (c) Concordance of top classified species among Sanger 16S, NGS 16S, Nanopore 16S and
561 reference standard.

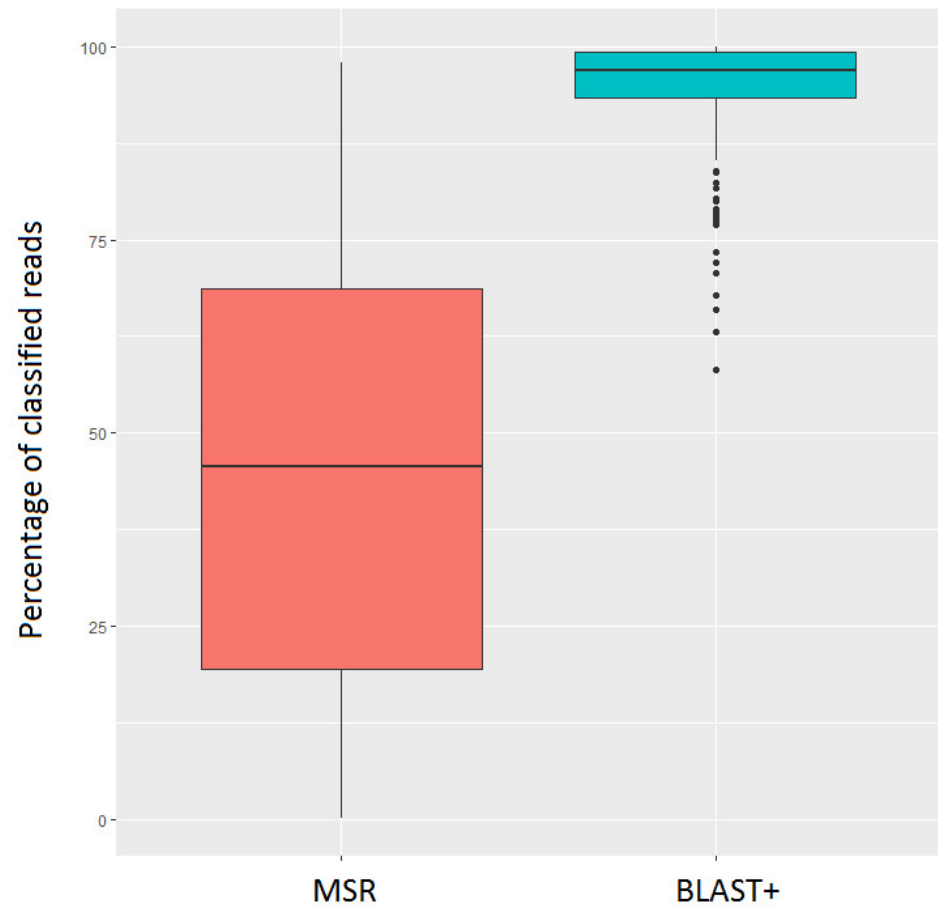
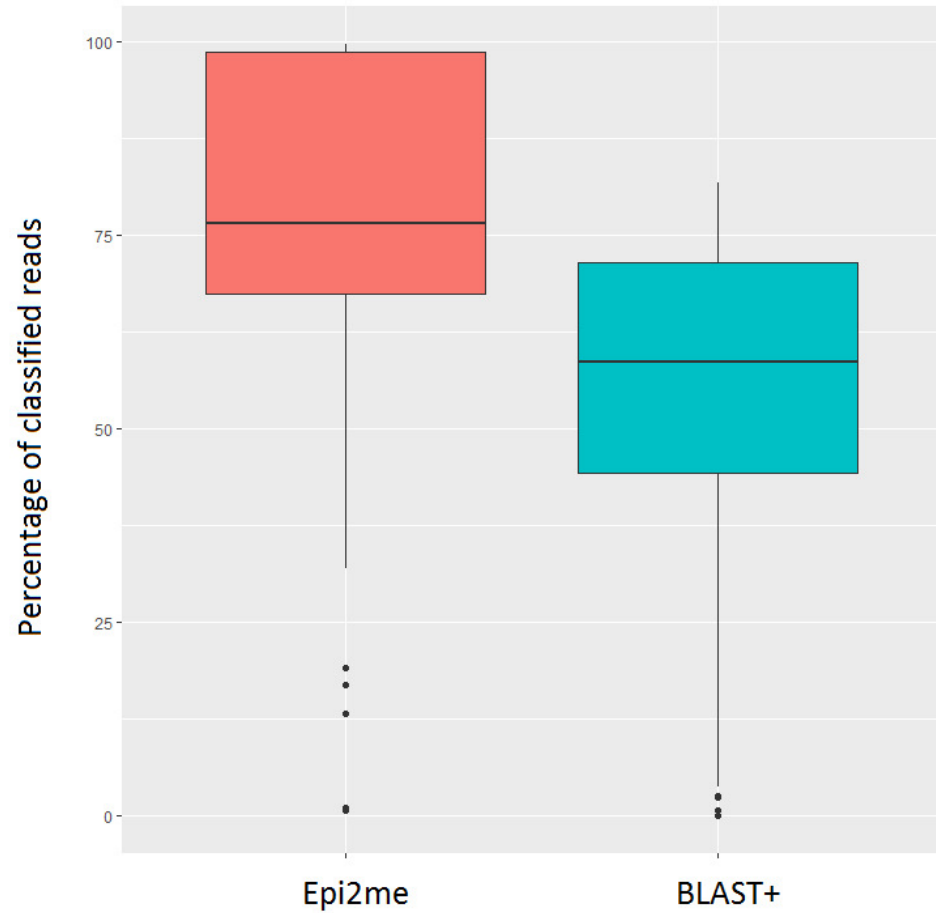
562

563
564
565
566
567
568
569
570

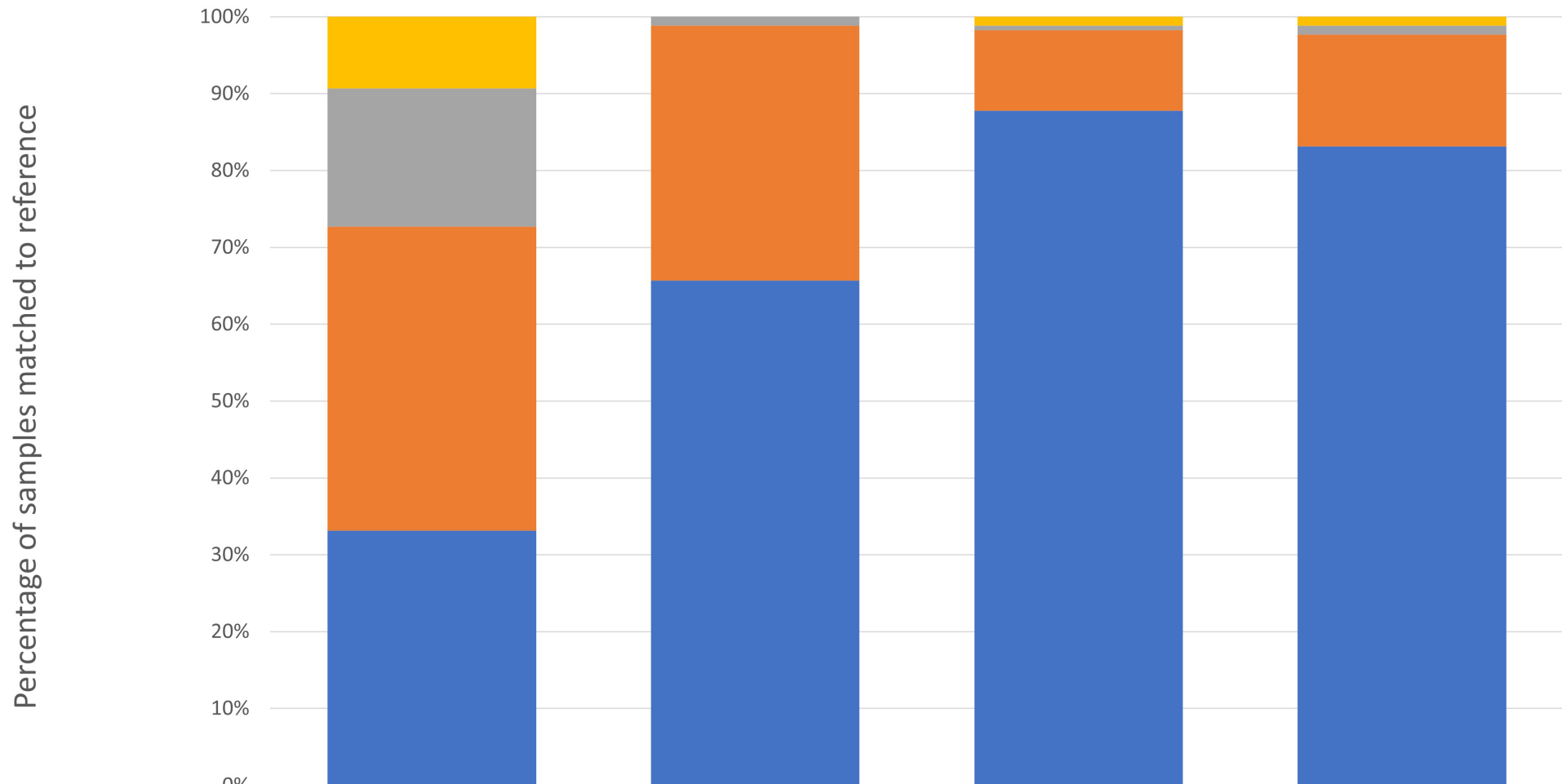


571
572
573

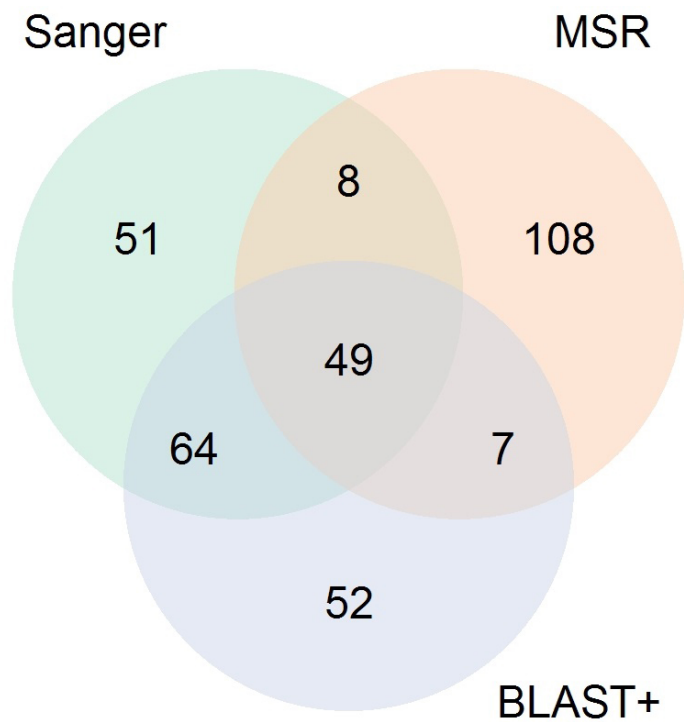
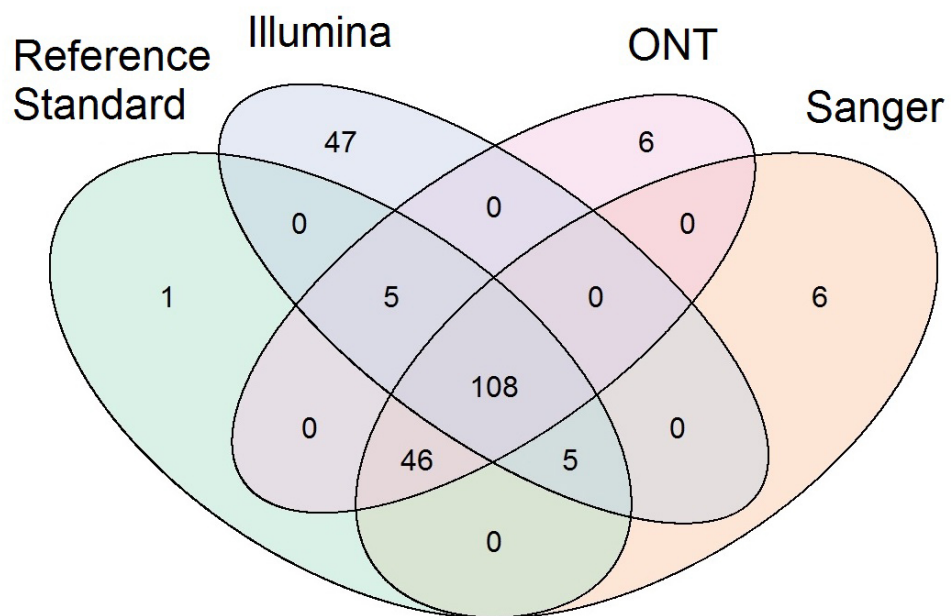
Figure 4. 16S rRNA gene sequencing workflow of the HTS technologies.

(a)**(b)**

The concordance between bacterial taxa generated from HTS technologies and the reference Sanger sequencing



	Miseq reporter (Illumina)	NGS_BLAST+ (Illumina)	Epi2me (Nanopore)	NanoBLAST+ (Nanopore)
Not match	9.30%	0.00%	1.16%	1.16%
Matched at family level	18.02%	1.16%	0.58%	1.16%
Matched at genus level	39.54%	33.14%	10.47%	14.54%
Matched at species level	33.14%	65.70%	87.79%	83.14%

(a)**(b)****(c)**

Illumina Sequencing

(16S Metagenomic Sequencing Library Preparation workflow)

DNA extraction and purification

Nanopore Sequencing

(16S Barcoding Kit 1 – 24)

78 hours

≥ 8.25 hours

172 samples/run

24 samples/run

Amplicon PCR and purification (4h)

Index PCR and purification (3h)

Bioanalyzer and qPCR (12h)

Library normalisation (2h)

Miseq sample loading (1h)

Sequencing and on-instrument analysis (56h)

Barcode PCR and purification (3h)

Quantification and pooling (1h)

Adapter ligation and sample loading (15min)

Sequencing (4h)

Basecalling (real-time)

Epi2me analysis (real-time)